Digital Object Identifier (DOI): 10.1109/APEC.2016.7468370

IEEE Applied Power Electronics Conference and Exposition (APEC), Long Beach, CA, USA, 2016

Frequency adaptive control of a smart transformer-fed distribution grid

Zhi-Xiang Zou
Giovanni De Carne
Giampaolo Buticchi
Marco Liserre

Suggested Citation

Z. Zou, G. De Carne, G. Buticchi and M. Liserre, "Frequency adaptive control of a smart transformer-fed distribution grid," *IEEE Applied Power Electronics Conference and Exposition (APEC)*, Long Beach, CA, 2016, pp. 3493-3499.

Frequency Adaptive Control of a Smart Transformer-Fed Distribution Grid

Zhi-Xiang Zou, Giovanni De Carne, Giampaolo Buticchi, Marco Liserre
Chair of Power Electronics
Christian-Albrechts University of Kiel
Kiel, Germany
zz, gdc, gibu, ml@tf.uni-kiel.de

***Abstract*—An advanced service provided by the Smart Transformer (ST) is the decoupling between the Medium Voltage (MV) and Low Voltage (LV) grids. In the LV side, the ST can modify the waveform's frequency in order to interact with the droop controllers of the local generators to control the power demand among the sources without affecting the MV grid. However, most of the existing controllers for power converters cannot guarantee good performances under variable frequency conditions. To address this issue, a frequency adaptive control scheme based on the Fractional-Order Repetitive Control (FORC) as well as Frequency Locked Loop (FLL) is proposed in this paper. This proposed scheme provides fast online parameter tuning capability in order to be highly adaptive to variable frequencies, and it can be implemented either in a ST converter or in distributed generators. In this work simulation and experimental results are provided to demonstrate the effectiveness and advantages of the proposed scheme.**

Keywords—Solid state transformer; distribution grid; frequency adaptive; frequency-locked loop; stability

I. INTRODUCTION

The increasing integration of Distributed Energy Resources (DERs) challenges the hosting capacity of distribution grids. As pointed out in recent literature, these intermittent distributed appliances will cause severe problems on the existing distribution grids in terms of voltage and current capacity limit violations, unintentional islanding, increased harmonic pollution, and reliability issue [1-3]. Moreover, these can propagate in other voltage level grids, like the MV ones. It is the case of the current imbalance in the LV grids, due to the presence of single-phase loads and generators, or voltage sags in the MV grids, that can affect sensitive loads in LV grids (*e.g.*, data center or high-precision electronic devices).

The ST, being a three-stage power electronics-based transformer, can be the solution to the aforementioned issues. In addition to transforming the voltage levels, it also provides ancillary services to the distribution grid, both in MV and LV side: improvement of the current and voltage profile [4], balancing services [5-6], and reliability improvement in the whole system [7]. In particular, the ST is able to decouple completely the LV grid from the MV grid thanks to the presence of the DC Link. While in the LV grid the ST controls the voltage waveform, in the MV grid it requests the active power demanded by the loads and regulates the injection of reactive power, (*i.e.* for voltage control). Of particular interest is the possibility to adapt the frequency to interact with the distributed generation [8] in order to change the power sharing between ST and distributed generation [9-10]. It is worth noticing that this solution has very limited impact on the main grid thanks to the electrical decoupling between the MV grid and LV grid.

Currently, most of the existing controllers for power electronics converters are designed to regulate signals with fixed fundamental frequency (*e.g.* 50/60 Hz signals) and offer accurate voltage/current control solutions [11]. However, in ST-fed distribution grid applications with variable frequency, these conventional control schemes incur in performance degradation [12-13]. To deal with this problem, the Fractional-Order Repetitive Control (FORC) plus Frequency Locked Loop (FLL)-based frequency adaptive control is proposed and implemented in both ST and DERs. Equipped with this proposed frequency adaptive control, the ST-fed distribution is able to modify online the power production and demand by changing the grid frequency while maintaining good performance.

This paper is organized as follows: the detailed frequency control of ST-fed distribution grid is given in Section II. In Section III, the stability of the control system is investigated considering the FLL. The proposed controller has been verified in Section IV with simulations performed in PLECS and experimental results have been performed in a Real Time Dynamic Simulator (RTDS) by means of the Control-Hardware-In-Loop (CHIL) method. Finally, conclusions are drawn in Section V.

II. FREQUENCY ADAPTIVE ST-FED DISTRIBUTION GRID

A. Frequency Control in Distribution Grid

Different from traditional distribution grid, the LV side voltage frequency of ST-fed distribution grid can be flexibly modified within a certain range according to the local grid codes (for example, ± 0.5Hz in Germany). Therefore, the power production and consumption of frequency-dependent appliances/loads can be adjusted as well following the frequency changes. Fig. 1 shows the power/frequency characteristics of DER and typical load in a distribution grid.

To mimic the power system inertia, the grid-interfaced power electronic converters usually adopt droop controllers reproducing the *P-f* droop behavior of synchronous generators used in the conventional power system [14-15]. The *P-f* droop curve with inductive output impedance is shown as the red curve in Fig. 1. Meanwhile, it is well known that the load magnitude (especially the motor load) is also strongly dependent on the system frequency as the blue curves. Within this context, the main reason to employ a frequency control is to reestablish the balance between power generation and load consumption. In the case of a load increment ΔP (for example, from load curve 1 to curve 2), if the distribution grid decreases its frequency from ω_1 to ω_2, the contribution of DER will increase while the load consumption will decrease. The frequency will continuously decrease until a new power balance between power production and consumption is established, and vice versa. Two main advantages are provided by the frequency control: 1) the current flow through the transformer can be limited to avoid overloads; 2) the power rating of controllable load or storage systems installed in a distribution grid can be partly reduced according to the droop coefficients of DERs and loads.

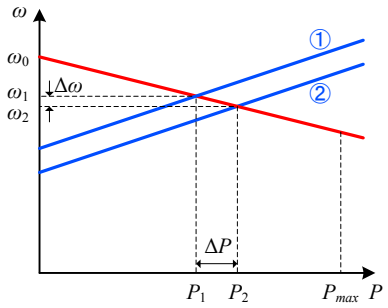

Fig. 1. Power/frequency characteristics of DER (red curve) and load (blue curves)

The simplified system configuration of the ST-fed distribution grid with the frequency control scheme is presented in Fig. 2. Droop control is employed both in ST and DER to provide frequency and power reference, respectively. In normal operation scenario, both the frequency and voltage amplitude of the LV side of the ST are kept constant at their nominal values. When the load increases, the frequency of LV side will be regulated following the droop curve as soon as the RMS current of ST exceeds the security limit. On the other hand, the variable frequency will be detected by the FLL of DER, whose dynamic response is much faster than the maximum rate of grid frequency [16]. According to the *P-f* droop curve, the DER is solicited to output desired real power/current under variable frequency condition.

B. Frequency Aaptive Control Strategy

To achieve good control performance, a frequency-adaptive voltage/current control scheme is proposed for both the ST LV side inverter and the DER grid-interfaced inverter. The overall control system is presented in Fig. 3(a), in which a FORC controller $G_{forc}(z^{-1})$ is plugged into the feed-forward channel of

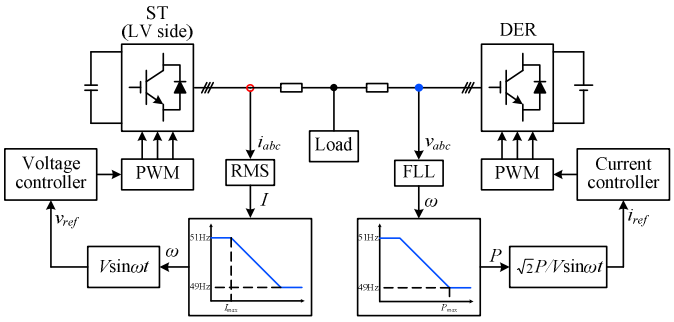

Fig. 2. Frequency control of a ST-fed distribution grid

the system. $G_c(z^{-1})$ and $G_p(z^{-1})$ are the transfer functions of conventional voltage/current controller, and control plant (DC/AC inverter); $R(z^{-1})$, $Y(z^{-1})$, and $D(z^{-1})$ are the reference, output, and disturbance of the control system; $E(z^{-1})$ and $U_r(z^{-1})$ are the tracking error and the FORC output. Study cases on the FORC-based system have been done in literature for several power applications, such as the grid-interfaced power converters [13], programmable AC power supply [12], active power filters [17], and active noise cancelations. The main idea of FORC controller is derived from Conventional Repetitive Control (CRC), whose transfer function is

$$G_r(z^{-1}) = k_r \frac{z^{-N}Q(z^{-1})}{1-z^{-N}Q(z^{-1})} \tag{1}$$

where k_r is the control gain; $Q(z^{-1})$ is the transfer function of a low-pass filter that improves the system stability; N is the order of CRC and can be expressed as f_s / f. Here, f_s and f are the sampling frequency and fundamental frequency, respectively. When f is fixed, a proper choice of f_s allows to make sure that N is an integer value. However, when the fundamental frequency is variable, the N would often be fractional in the case of fixed sampling rate. A fractional order N which indicates a Fractional Delay (FD) cannot be directly implemented in the practical digital controller. To address this issue, the FORC with a fixed sampling rate is proposed and the schematic diagram of the proposed control system is shown in Fig. 3(b), where $G_f(z^{-1})$ is the transfer functions of a phase lead compensation filter, N_i and F are the integral and fraction orders of FORC ($N = N_i + F$).

As mentioned before, the main problem is to properly deal with the potential FD in a FORC system caused by the time-varying fundamental frequency. According to the FD filters design method [18-19], the FD z^{-F} of Fig. 3(b) can be approximated by a Lagrange Interpolation polynomial Finite-Impulse-Response (FIR) filter as following

$$z^{-F} \approx \sum_{k=0}^{n} A_k z^{-k} \tag{2}$$

where $k \in \mathbf{N}$, and the Lagrange coefficient A_k of (2) can be calculated as

$$A_k = \prod_{\substack{i=0 \\ i\neq k}}^{n} \frac{F-i}{k-i}, \qquad k,i = 0,1,\ldots,n. \tag{3}$$

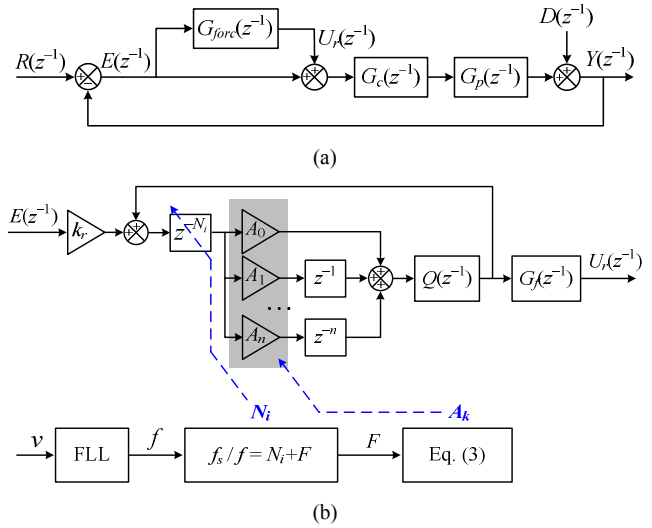

Fig. 3. Schematic diagram of frequency adaptive control system: (a) overall control system, (b) FORC

Substituting (2) and (3) into (1), the transfer function of FORC will be obtained as following

$$G_{forc}(z^{-1}) = \frac{U_r(z^{-1})}{E(z^{-1})} = k_r \frac{z^{-N_i}\sum_{k=0}^{n} A_k z^{-k} Q(z^{-1})}{1 - z^{-N_i}\sum_{k=0}^{n} A_k z^{-k} Q(z^{-1})} G_f(z^{-1}) \quad (4)$$

According to the properties of the Lagrange Interpolation polynomial, there is always an approximation remainder between the theoretical FD and the polynomial. The remainder term of FD can be written as follows

$$R_n = z^{-F} - \sum_{k=0}^{n} A_k z^{-k} = \frac{\xi^{-F-n}\prod_{i=0}^{n-1}(-F-i)}{(n+1)!}\prod_{i=0}^{n}(F-i) \quad (5)$$

where $\xi \in [T_k, T_{k+1}]$ with T_k and T_{k+1} being the kth and $k+1$th sampling intervals, respectively. Fig. 4(a) compares the magnitude responses of Lagrange Interpolation-based FD with different polynomial degrees. With the increase of the polynomial degree n, better approximation accuracy can be achieved. It can be seen that the approximated FIR filter with the degree $n \geq 2$ can achieve a good approximation towards the FD z^{-F} within the Nyquist frequency. For example, the magnitudes are close to the nominal value (abs = 1) within the bandwidth of 75% Nyquist frequency when $n = 3$, which indicates the proposed FORC can exactly track fractional period signals within the frequency range. To evaluate the tracking ability, the approximation remainder norms of FORC with different sampling frequencies are analyzed as shown in Fig. 4(b) and also compared with those of CRC. When the fundamental frequency varies in a certain range, the remainder norms of CRC change drastically and some of them are relatively high, indicating the tracking error could not be eliminated under variable frequency condition. However, the norms of FORC always remain in a lower level at the neighborhood of fundamental frequency. In addition, the averaging norm at the frequency neighborhood will decrease when the sampling frequency increases. It can be concluded that a higher sampling frequency should be employed to reduce the RMS value of tracking error of FORC or CRC.

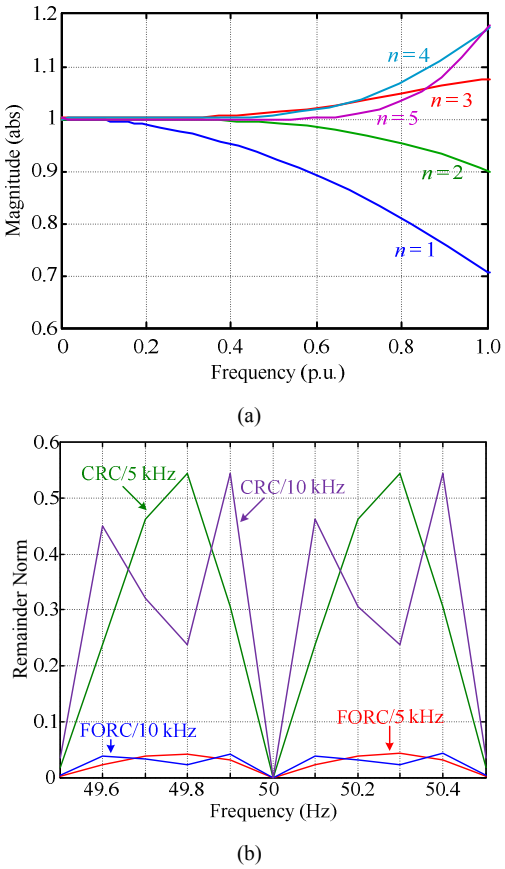

Fig. 4. Performance evaluation: (a) magnitude response of Lagrange Interpolation-based FD with different degrees, and (b) comparisons of remainder norm between CRC and FORC under different sampling frequencies

The FORC scheme provides a general approach to track or eliminate of any periodic signal with an arbitrary fundamental frequency and fixed sampling frequency. It is evident that the transfer function (4) becomes a conventional repetitive control as (1) in the case of an integral order ($F = 0$). From Fig. 3(b), it is shown that two different time scales have been utilized in the control system: 1) the changing rate of delay orders (N_i and F) is highly dependent on the dynamic response of frequency detector, *e.g.* FLL in this case; 2) the update rate of A_k depends on the sampling frequency. In the distribution grid control applications, both N_i and F change relatively slowly compared with the sampling rate of the FORC system. Moreover, the Lagrange Interpolation-based FD only needs a small number of sums and multiplications for a fast online update of A_k so that it can be easily implemented in the real-time control system along with high approximation accuracy.

III. Stability Analysis

A. System Stability without FLL

The closed-loop transfer function of the frequency adaptive control system can be derived from Fig. 3(a). Before the FORC

plugs in, the transfer function of the former closed-loop system is

$$H(z^{-1}) = \frac{Y(z^{-1})}{R(z^{-1})} = \frac{G_c(z^{-1})G_p(z^{-1})}{1+G_c(z^{-1})G_p(z^{-1})} \tag{6}$$

When the FORC is employed, the error transfer function of the overall system can be derived as following

$$\begin{aligned} G_e(z) &= \frac{E(z^{-1})}{R(z^{-1})-D(z^{-1})} \\ &= \frac{(1-z^{-N_i}\sum_{k=0}^{n}A_k z^{-k})\cdot(1+G_c(z^{-1})G_p(z^{-1}))^{-1}}{1-z^{-N_i}\sum_{k=0}^{n}A_k z^{-k}Q(z^{-1})(1-k_r G_f(z^{-1})H(z^{-1}))} \end{aligned} \tag{7}$$

From (7), the FORC-based frequency adaptive control system is asymptotically stable if the following two conditions hold: 1) the roots of $1 + G_c(z^{-1})G_p(z^{-1}) = 0$ are inside the unity circle; 2) the roots of $1-z^{-N_i}\sum_{k=0}^{n}A_k z^{-k}Q(z^{-1})(1-k_r G_f(z^{-1}) \cdot H(z^{-1}))$ are inside the unity circle.

The first stability condition requests the former closed-loop system to be stable before the FORC plugs in. The second stability condition can be rewritten as

$$\begin{aligned} \left\|1-k_r G_f(z^{-1})H(z^{-1})\right\| &< \left\|Q(z^{-1})\cdot\sum_{k=0}^{n}A_k z^{-k}\right\|^{-1} \\ &\le \left\|Q(z^{-1})\right\|^{-1}\cdot\left\|\sum_{k=0}^{n}A_k z^{-k}\right\|^{-1} \end{aligned} \tag{8}$$

As seen from Fig. 4(b), the magnitudes of FIR filters are always closed to 1 within the band-pass, so that

$$\left\|\sum_{k=0}^{n}A_k z^{-k}\right\|^{-1} \approx \left\|\sum_{k=0}^{n}A_k z^{-k}\right\| \to 1 \tag{9}$$

Substituting (9) into (8), it can be seen that the stability condition of FORC-based system turns to be the same as that of CRC systems. Moreover, considering that the characteristics of the proposed FD filter is way similar to that of $Q(z^{-1})$, the low-pass filter can be omitted in some special cases. For example, when the designed bandwidth of FD is close to the cut-off frequency of $Q(z^{-1})$, $\left\|Q(z^{-1})\right\|\cdot\left\|\sum_{k=0}^{n}A_k z^{-k}\right\| \approx \left\|\sum_{k=0}^{n}A_k z^{-k}\right\|$ within the cut-off frequency/bandwidth. In this regard, the stability condition of FORC-based system is still fulfilled without the need of $Q(z^{-1})$. In the normal conditions, since the cut-off frequency of $Q(z^{-1})$ is usually lower than the bandwidth of the FD, the characteristics of $Q(z^{-1})$ is more decisive to the system stability. With this consideration, most of design criteria of the well-known CRC-based systems can be also used for the FORC analysis and design.

B. System Stability with FLL

As discussed in Section III-B, a FLL is employed in DER to provide the real-time measurement of frequency for the online update of the Lagrange coefficients. With properly designed parameters, FLL can provide faster dynamic response than other phase locked loops under variable frequency conditions [20]. For example, the gains of FLL $k = \sqrt{2}$ and $\gamma = 100$ are used in our system and the detailed characteristics are shown in TABLE I.

TABLE I. CHARACTERISTICS OF FLL

Parameter	Value
Nominal frequency	50 Hz
Settling time	45 ms
Overshoot (to nominal value)	3.1 %
Frequency range	47~52 Hz

According to the FLL characteristics, the settling time is around 50ms which is much faster than the maximum rate of grid frequency variation (*e. g.* 1 Hz/s) and much slower than the sampling frequency of the current loop of DER system (typically from 5 kHz to 20 kHz). Considering a 5 kHz sampling frequency system as an example, in case of 1 Hz frequency variation, the FLL takes 500 ms to increase or decrease the order of integer delay N_i by 1, and at the same time the order of fractional delay would change only 4×10^{-4} over one sampling interval. Substituting this value of 4×10^{-4} into (3), the variations of A_k are less than 1×10^{-4}. In other words, the change of the Lagrange coefficients in one sampling interval is negligible so that has very limited effects on the FORC output As a result, the overall control system can be treated as a Linear Time-Invariant (LTI) system in the stability analysis. With these considerations, a schematic diagram of the overall system is shown in Fig. 5, where an outer-loop incorporating the FLL is added, and the input signal R is the amplitude of the reference, v_{pcc} is the PCC voltage.

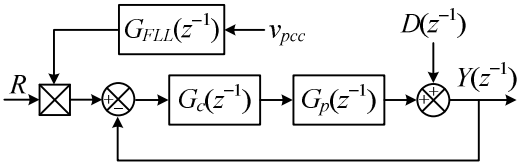

Fig. 5. Block diagram of DER control system with FLL

It is worth noting that the stability conditions in Section III-A are derived from the generic closed-loop system so that they are still applicable to the FLL-considered system. However, the closed-loop transfer function of (6) needs to be revised as following:

$$Y(z^{-1}) = H(z^{-1})G_{FLL}(z^{-1})\cdot R\cdot v_{pcc} \tag{10}$$

where $G_{FLL}(z^{-1})$ is the transfer function of FLL and its *s*-domain representation is given in (11). From [16], it can be seen that the FLL behaves as a nonlinear system. To obtain the transfer function, linearization procedure must be carried out and the transfer function can be derived as follows

$$G_{FLL}(s) = \frac{k^2\omega_0 s}{s^3 + k\omega_0 s^2 + \omega_0^2 s + k\gamma\omega_0} \quad (11)$$

where k and γ are the gains of FLL, which are $\sqrt{2}$ and 100, respectively, for the 47-52Hz applications, ω_0 is the fundamental frequency with 50Hz. Discretizing (11) and substituting that into (10), a pole-map can be drawn based on the transfer function of (10) and shown in Fig. 6. Compared with the pole-map of the control system without FLL, three additional poles (red poles) are introduced and are on the left half plane which fulfills the first stability condition. It can be seen that the system with a FLL has lower bandwidth but better rejection of grid disturbances.

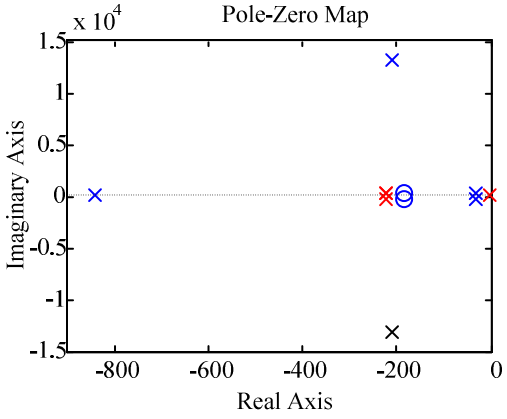

Fig. 6. Pole-zero map of the overall control system with FLL: closed-loop system poles without FLL (blue crosses), FLL additional poles (red crosses)

IV. Simulation and Experimental Verifications

This section provides the simulation results obtained implementing the CRC and FORC control in MATLAB and the verification of the proposed method with the Control-Hardwar-In-Loop technique by means of a Real Time Digital Simulator.

A. Simulation Results

To validate the proposed strategy, the ST-fed distribution grid of Fig. 2 has been simulated. The nominal voltage of ST LV side is 230V (RMS), 50Hz, and the security limit of the ST LV side current is set as 14.2A (RMS) in this study case. As first approximation, it has been assumed that both the voltage and current of ST LV side are sinusoidal, thus the RMS values are adopted for the thresholds of frequency control. The power generation of DER is 3.5kW (Power Factor (PF) = 1) at the nominal frequency, and it is connected to the Point of Common Coupling (PCC) via a feeder, whose line impedance is Z_g = 0.03 + j0.06 Ω. The total load demand is 7kW (PF = 0.85), while the linear load and nonlinear load demands are both 3.5kW. At t = 0.5s, the total load demand increases from 7kW to 8.75kW. As soon as the ST LV side current exceeds the security limit, the frequency control is activated. As shown in Fig. 7(a), the current of the ST LV side decreases till below the security limit and reaches its new steady-state by means of frequency control. At the same time, the voltage amplitude of ST reverts to its normal state in less than one cycle and remains the same during all the frequency control stage. Fig. 7(b) shows frequency and power production details during the frequency control stage. When the load increases, the frequency reference of ST LV side voltage starts to decrease (with the rate of 0.28Hz/sec) instantaneously in order to reestablish the power balance within the distribution grid. After the frequency drop, the FLL can fast and accurately respond to the frequency variation and provides good frequency performance to the DER. Following the frequency, the power production of DER proportionally increases according to the given *P-f* droop curve. At t = 1.2s, the power balance of the distribution grid is established again and the final frequency holds the line of 49.8Hz.

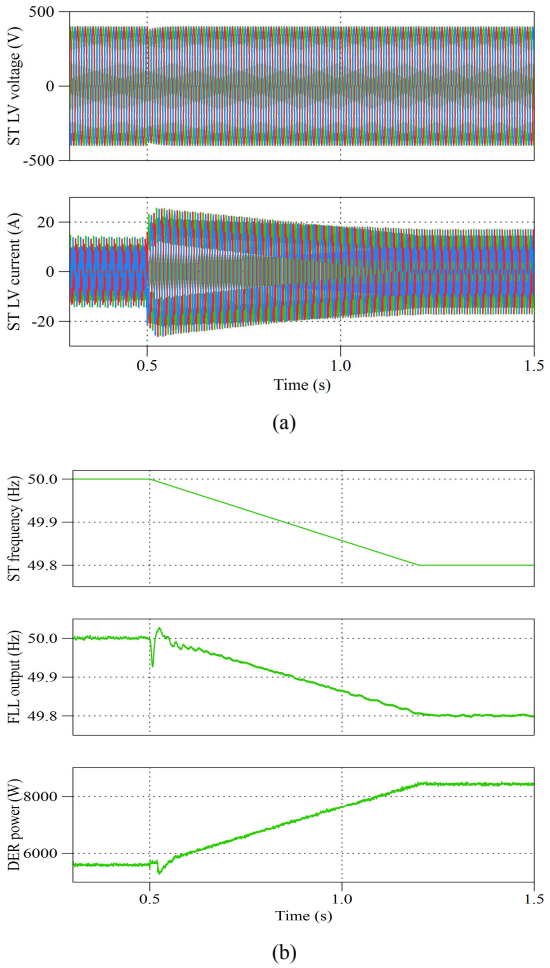

Fig. 7. The ST-fed distribution grid with frequency control: (a) ST LV side voltage and current, (b) reference frequency of ST LV voltage, freuqnecy detected by FLL of DER, and DER output power (from top to bottom)

Fig. 8 shows the performance comparisons of the ST-fed distribution grid at the neighboring frequency around 49.8Hz when different control strategies are used. In the first case, conventional repetitive controllers are employed in both the ST voltage controller and the DER current controller. From Fig. 8(a) and (b), it is clear that the ST voltage and the DER current contain considerable harmonics under variable frequency condition. In the second case, the proposed FORC controllers are implemented in the ST voltage controller and the DER current controller. Although a considerable amount of

nonlinear loads are connected to the grid, the FORC enables the ST and the DER to provide much better quality sinusoidal voltage and current and offers very good voltage/current harmonic mitigation capacity. Generally speaking, Fig. 8(c) and (d) demonstrate that the FORC is adaptive to frequency variation, whereas conventional controllers are not.

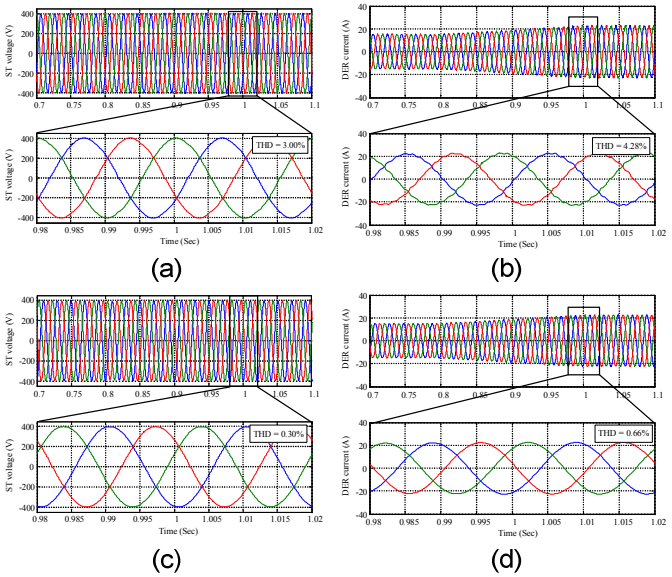

Fig. 8. Voltage/Current waveforms of a ST-fed distribution grid during the frequency control: (a) CRC-controlled ST LV side voltage, (b) CRC-controlled DER output current, (c) FORC-controlled ST LV side voltage, and (d) FORC-controlled DER output current

B. Experimental Results

The effectiveness of the FORC controller has been validated experimentally by means the Control Hardware In-Loop method using RTDS. This method allows simulating the converter behavior using a real controller implemented in an external device. The lab facility that performs this experiment is shown in Fig. 9. The voltage measurement at the ST bus are taken from the RTDS and sent to the dSPACE, where the control is implemented. The dSPACE system reads the new voltage measurements and generates the PWM signals for RTDS by the designed controller. Here the PWM signals are directly imposed to the ST LV side simulated in a small-time step subsystem. This enables a more realistic simulation of the power semiconductors, due to the reduced time steps (1-2 µs) with respect to the main grid (50 µs). The LV grid implemented in RTDS is a modified European LV distribution network benchmark [21], shown in Fig. 9 as well. With respect to the original grid the loads are balanced and the wind turbine has been neglected in order to reduce the computational effort in RTDS. The controls of local PV and battery systems have been simplified and the frequency-adaptive control scheme and FLL have not been utilized in this grid. The effectiveness of the proposed method has been proved in presence of disturbances, as a three-phase 5th harmonic current source of 10 A, simulating a non-linear load, installed at the bus 14.

The experimental results have been carried out comparing the performances of the CRC and the FORC in nominal conditions (50 Hz) and with lower grid frequency (49.8 Hz).

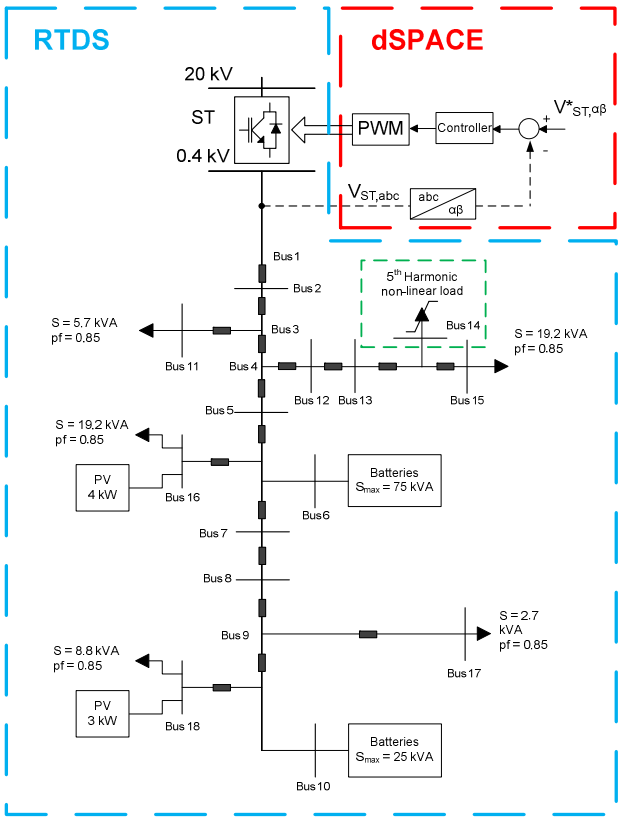

Fig. 9. Modified CIGRE European LV distribution network benchmark implemented in RTDS (blue square), LV side ST control implemented in dSPACE (red square), 5th harmonic non-linear load (green square)

As can be noticed from Fig. 10(a) and (c), where the voltage waveforms over a time window of 40 ms have been plotted, the CRC and the FORC have comparable performances at the nominal frequency. When the frequency changes, the performance of the two methods differs substantially, as shown in Fig 10(b) and (d). The CRC causes the voltage waveform to decrease its amplitude *e.g.* 290. When the FORC is implemented in the ST control the amplitude is kept to the nominal value of 325V peak and no harmonic content is present in the voltage waveform. Similar consideration can be drawn from the current waveform analysis. Although the performance is similar at the nominal frequency, Fig. 11(a) and (c), the amplitude of the current is heavily affected when the CRC is applied.

Taken in account the constant impedance nature of the loads installed in the simulated grid, a lower voltage value leads to a lower current request from the loads, affecting the power quality. When the FORC is employed as controller, the current has the same amplitude of the 50 Hz case, guaranteeing the same power quality standard like the 50 Hz case.

V. CONCLUSIONS

This paper proposed a frequency-adaptive ST-fed distribution grid. In this scenario, the ST is able to flexibly modify the LV side frequency with the purpose of avoiding overload and reducing the power rating of controllable load or storage system. The proposed FORC technology ensures better

performance of the ST and the power electronics interfaced-DERs in the distribution grid under variable frequency condition. Comprehensive control design and stability analysis considering FLL are presented in this paper. A study case of the proposed frequency-adaptive ST-fed distribution grid is performed in both the simulation and experiment platform. The results prove the power sharing ability of frequency-adaptive ST-fed distribution grid and the effectiveness of the proposed control strategy under variable frequency conditions.

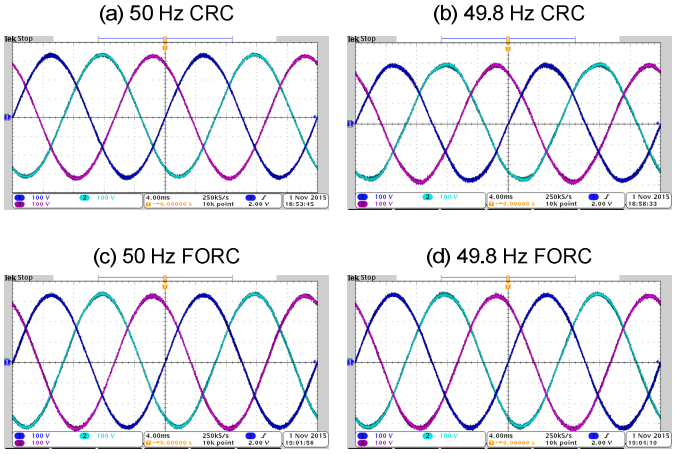

Fig. 10. Voltage waveforms of a ST-fed distribution grid during the frequency control: (a) CRC 50Hz, (b) CRC 49.8 Hz, (c) FORC 50Hz, and (d) FORC 49.8 Hz

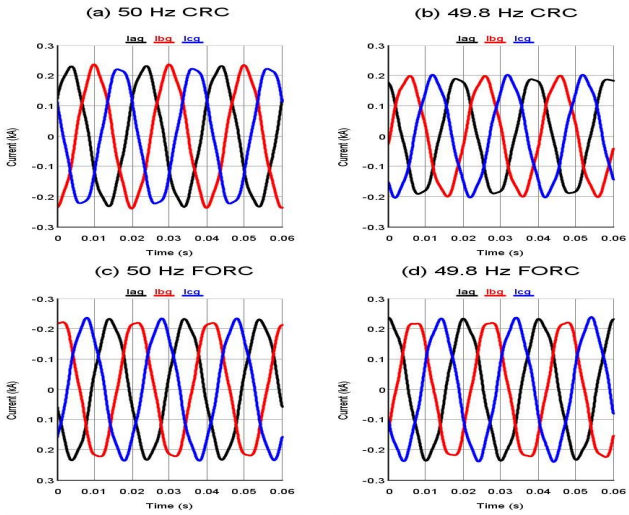

Fig. 11. Current waveforms of a ST-fed distribution grid during the frequency control: (a) Classical Control 50Hz, (b) Classical Control 49.8 Hz, (c) FORC 50Hz, and (d) FORC 49.8 Hz

REFERENCES

[1] A. Bhowmik, A. Maitra, S.M. Halpin, and J.E. Schatz, "Determination of allowable penetration levels of distributed generation resources based on harmonic limit considerations," *IEEE Transactions on Power Delivery*, vol. 18, no. 2, pp. 619-624, Apr. 2003.

[2] V.H.M. Quezada, J.R. Abbad, and T.G.S. Román, "Assessment of energy distribution losses for increasing penetration of distributed generation," *IEEE Transactions on Power Systems*, vol. 21, no. 2, pp. 533-540, May 2006.

[3] E.J. Coster, J.M.A. Myrzik, B. Kruimer, and W.L. Kling, "Integration issues of distributed generation in distribution grids," *Proceedings of the IEEE*, vol. 99, no. 1, pp. 28-39, Jan. 2011.

[4] G. De Carne, M. Liserre, K. Christakou, and M. Paolone, "Integrated voltage control and line congestion management in active distribution networks by means of smart transformers," in *IEEE 2014 International Symposium on Industrial Electronics*, 2014, pp. 2613-2619.

[5] G. De Carne, G. Buticchi, M. Liserre, C. Yoon, and F. Blaabjerg, "Voltage and current balancing in low and medium voltage grid by means of smart transformer," in *IEEE 2015 Power & Energy Society General Meeting*, 2015, pp. 1-5.

[6] C. Kumar and M. Liserre, "Operation and control of smart transformer for improving performance of medium voltage power distribution system," in *IEEE 6th International Symposium on Power Electronics for Distributed Generation Systems*, 2015, pp. 1-6.

[7] A.Q. Huang, M.L. Crow, G.T. Heydt, J.P. Zheng, and S.J. Dale, "The future renewable electric energy delivery and management (FREEDM) system: The energy internet," *Proceedings of the IEEE*, vol. 99, no. 1, pp. 133-148, Jan. 2011.

[8] G. Buticchi, M. Liserre, D. Barater, C. Concari, A. Soldati, and G. Franceschini, "Frequency-based control of a micro-grid with multiple renewable energy sources," in *IEEE 2014 Energy Conversion Congress and Exposition*, 2014, pp. 5273-5280.

[9] G. De Carne, G. Buticchi, M. Liserre, and C. Vournas, "Frequency-based overload control of smart transformers," in *IEEE 2015 PowerTech*, 2015, pp. 1-5.

[10] G. De Carne, G. Buticchi, M. Liserre, P. Marinakis, and C. Vournas, "Coordinated frequency and voltage overload control of smart transformers," in *IEEE 2015 PowerTech*, 2015, 1-5.

[11] J. Rocabert, A. Luna, F. Blaabjerg, and P. Rodríguez, "Control of power converters in AC microgrids," *IEEE Transactions on Power Electronics*, vol. 27, no. 11, pp. 4734-4749, Nov. 2012.

[12] Z. Zou, K. Zhou, Z. Wang, and M. Cheng, "Fractional-order repetitive control of programmable AC power sources," *IET Power Electronics*, vol. 7, no. 2, pp. 431-438, Mar. 2015.

[13] Y. Yang, K. Zhou, H. Wang, F. Blaabjerg, D. Wang, and B. Zhang, "Frequency adaptive selective harmonic control for grid-connected inverters," *IEEE Transactions on Power Electronics*, vol. 30, no. 7, pp. 3912-3924, Jul. 2015.

[14] R. Brandt, "Theoretical approach to speed and tie line control," *Transactions of the American Institute of Electrical Engineers*, vol. 66, no. 1, pp. 24-30, Jan. 1947.

[15] N. Cohn, "Recollections of the evolution of realtime control applications to power systems," *Automatica*, vol. 20, no. 2, pp. 145-162, Mar. 1984.

[16] P. Rodríguez, A. Luna, I. Candela, R. Mujal, R. Teodorescu, and F. Blaabjerg, "Multiresonant frequency-locked loop for grid synchronization of power converters under distorted grid conditions," *IEEE Transactions on Industrial Electronics*, vol. 58, no. 1, pp. 127-138, Jan. 2011.

[17] Z. Zou, K. Zhou, Z. Wang, and M. Cheng, "Frequency-adaptive fractional-order repetitive control of shunt active power filters," *IEEE Transactions on Industrial Electronics*, vol. 62, no. 3, pp. 1659-1668, Mar. 2015.

[18] T. I. Laakso, V. Valimaki, M. Karjalainen, and U. K. Laine, "Splitting the unit delay," *IEEE Signal Processing Mag.*, vol. 13, no. 1, pp. 30–60, Jan. 1996.

[19] Y. Wang, D. Wang, B. Zhang, and K. Zhou, "Fractional delay based repetitive control with application to PWM DC/AC converters," in *16th IEEE International Conference on Control Applications*, 2007, pp.928-933.

[20] R. Teodorescu, M. Liserre, and P. Rodríguez, *Grid converters for photovoltaic and wind power systems*, Wiley, Chichester, 2011.

[21] "*Benchmark system for network integration of renewable and distributed energy resources c06.04.02*," CIGRE, Tech. Rep., 2014.